NRL Report 7579

Use of a Self-Focusing Antenna for Low-Angle Tracking

JAMES H. HUGHEN

Radar Analysis Branch
Radar Division

June 28, 1973

NAVAL RESEARCH LABORATORY
Washington, D.C.

CONTENTS

Abstract ii
Authorization ii

INTRODUCTION 1

MATHEMATICAL DEVELOPMENT 2

General Case 2
Case of Two Subapertures 3

RESULTS 4

CONCLUSIONS 9

ACKNOWLEDGMENT 9

REFERENCES 10

APPENDIX — Computer Simulation Program for the Self-Focusing Problem 11

ABSTRACT

The response of a self-focusing antenna to two closely spaced point targets is investigated. The geometry simulated corresponds to the radar tracking of a low-flying target over a reflective surface. In one case the antenna consists of a vertical linear array of elements. When the conjugates of the incident signals are retransmitted at each element, after several iterations the antenna radiation pattern introduces significant discrimination against the weaker of the two unresolvable point targets. In the other case the same aperture is divided into two equal subapertures, and conjugate reflections are applied to the two subapertures rather than to each element. It is found that very nearly the same weak-target discrimination results. The implications of these results with regard to low-angel tracking are discussed.

AUTHORIZATION

NRL Problem R02-59
Project RF-12-151-402-4015

Manuscript submitted March 16, 1973.

USE OF A SELF—FOCUSING ANTENNA FOR LOW—ANGLE TRACKING

INTRODUCTION

In the radar tracking of an object positioned over a reflective surface, a reflection from the surface may appear to the radar to be an image below the surface. (See Fig. 1, taken from Ref. 1.) If the energy from the image falls within the main lobe of the tracking radar, severe errors can result. There have been a number of attempts to reduce these errors (for some examples see Ref. 2), but the problem is still an open one. This report discusses the feasibility of using an adaptive or self-focusing antenna for low-angle tracking.

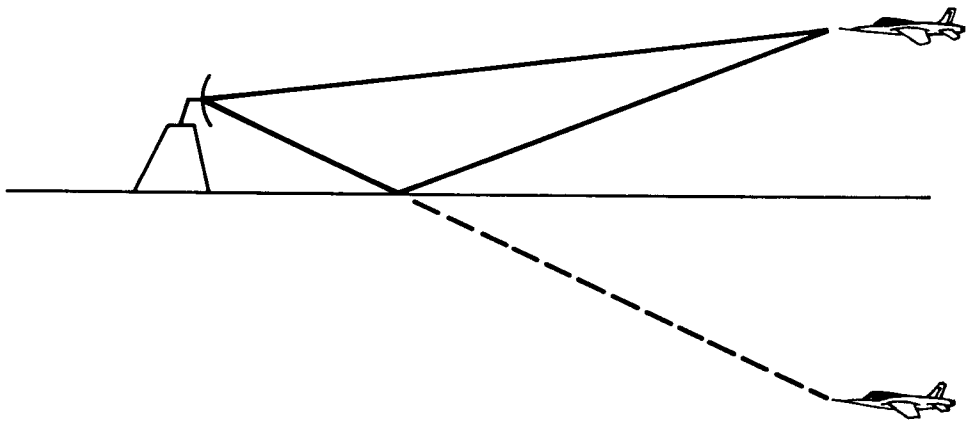

Fig. 1 — Reflection from the surface appears as a target image

A self-focusing antenna uses the unique properties of conjugate reflections to return, as a coherent wavefront, an incident wavefront in the direction from whence it came. If the incident waveform is backscatter from two point targets, the retransmitted wave is directed toward the stronger target, thus discriminating against the weaker target (3-5). It is this discrimination against a weaker target which could render this technique useful for low-angle tracking.

At the time this investigation was begun, it was well known (5) that discrimination against a weaker target would occur if sufficient aperture were available to resolve the targets. However, if self-focusing is to be useful for low-angle tracking, discrimination against a weaker target, i.e., the image, must occur when the target and image lie within the main-lobe beamwidth. This is the main question to which the investigation reported on here was addressed.

MATHEMATICAL DEVELOPMENT

General Case

A computer simulation program, provided as an appendix, was developed to calculate and plot the radiation intensity at points in the target/image plane. Plotting the radiation pattern proved to be a convenient way to analyze the behavior of the self-focusing antenna for closely spaced targets. The geometry used in the simulation program is shown in Fig. 2. The self-focusing antenna consists of a linear aperture D sampled at every half wavelength. The sample points x_i are a measure of distance above the reference plane (ocean surface). The number of aperture samples actually used in the program was 51. The distance from the antenna to the target axis is R, and the target height is h_t. The radiation intensity is calculated at discrete points u_j along the target/image axis. The distance d_{ij} from a sample point x_i along the aperture to a sample point u_j on the target/image axis is

$$d_{ij} = \sqrt{R^2 + (x_i - u_j)^2}, \tag{1}$$

and the corresponding electrical length of that path is

$$\phi_{ij} = \frac{2\pi}{\lambda} d_{ij}, \tag{2}$$

where λ is the wavelength. Neglecting all attenuation losses, a complex transmission coefficient Γ_{ij} for the ijth path can be defined as the complex exponent ϕ_{ij}, i.e.,

$$\Gamma_{ij} = e^{j\phi_{ij}}, \; j > \frac{N}{2}, \tag{3a}$$

where N is the total number of sample points along the target/image axis. For paths which include a surface reflection, an additional 180° phase shift is included, i.e.,

$$\Gamma_{ij} = e^{j(\phi_{ij} + \pi)}, \; j = 1, 2, \ldots \frac{N}{2}. \tag{3b}$$

The attenuation of the surface reflection could be accounted for in the coefficient Γ_{ij}; however, in the present program this attenuation is accounted for by reducing the cross section of the image. There is a radar cross section $\rho(u_j)$ (a complex number) associated with each sample point along the target/image axis, but only the nonzero points correspond to the target and its image.

The process is begun by illuminating each point along the target axis with some initial function $B_0\ (u_j)$ which was taken to be uniform, i.e., unity for all j. On the first iteration, the wave back at the ith sample point in the aperture is given by

$$A_1\ (x_i) = \sum_j B_0\ (u_j)\ \rho\ (u_j)\ \Gamma_{ij}. \tag{4}$$

The paths are assumed to be reciprocal, that is $\Gamma_{ji} = \Gamma_{ij}$. At each point x_i in the aperture, the complex conjugate $A_1^*\ (x_i)$ is generated and transmitted. This is the essential operation constituting self-focusing. In practical terms, at each sample point in the aperture, the phase of the received signal is reversed and then retransmitted. Back at the target/image axis, the wave at each point is

$$B_1(u_j) = \sum_i A_1^*(x_i)\,\Gamma_{ij}, \tag{5}$$

or substituting Eq. (4) into Eq. (5),

$$B_1(u_j) = \sum_i \left[\sum_k B_0^*(u_k)\,\rho^*(u_k)\,\Gamma_{ik}^*\right]\Gamma_{ij}. \tag{6}$$

The subscript one on $B_1(u_j)$ indicates the first iteration. After iterating this process a number of times, results converge to form the adapted or focused pattern.

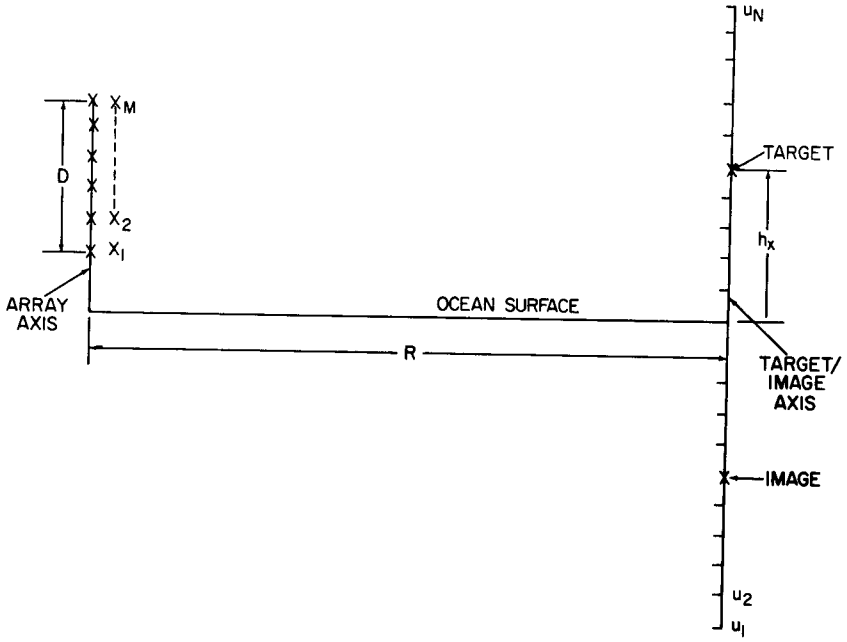

Fig. 2 — Geometry used in simulation program

Case of Two Subapertures

A variation on the previous approach, which can lend considerable practicability to the concept of self-focusing, involves the phasing of two subapertures rather than the phasing of each element of an array. Two subapertures are formed by dividing the aperture D in Fig. 2 into halves. Now instead of retransmitting the conjugate of the signals received at each sample point in the aperture, the average phase across the aperture is computed, conjugated, and retransmitted. On retransmission the phase across the subaperture is constant. In effect then, the phase distribution across the entire aperture is replaced by a two-step approximation. The average signal for the first subaperture is

$$E_k = \frac{2}{M}\sum_{i=1}^{M/2} A_k(x_i), \tag{7}$$

where M is the total number of sample points in the aperture D and k is the iteration number. For the second subaperture,

$$F_k = \frac{2}{M} \sum_{i=\frac{M}{2}+1}^{M} A_k\ (x_i). \tag{8}$$

Then the wave at a point on the target/image axis is (kth iteration)

$$B_k\ (u_j) = \sum_{i=1}^{M/2} E_k^*\ \Gamma_{ij} + \sum_{i=\frac{M}{2}+1}^{M} F_k^*\ \Gamma_{ij}$$

$$= E_k^* \sum_{i=1}^{M/2} \Gamma_{ij} + F_k^* \sum_{i=\frac{M}{2}+1}^{M} \Gamma_{ij}. \tag{9}$$

Some performance degradation is expected to result from this approach, but if the phase distribution across the entire aperture is benign enough, very little degradation will occur. This is the second major question to which this brief study was directed.

RESULTS

The magnitude $|\ B_k\ (u_j)\ |$ of the wave is computed and plotted at 51 points along the target/image axis. (The plot routine interpolates linearly between computed points.) In Fig. 3 the distance between the target and its image corresponds approximately to the 3-dB beamwidth of the antenna. The arrows at 1000 m and −1000 m locate the target* and image respectively and also indicate their relative strengths. A distinct increase in image discrimination can be seen for the second iteration (Fig. 3b), and for the fifth iteration (Fig. 3c) the image is completely nulled out. Positioning of a null exactly on the image is not possible in general, but it occurs here because the separation between the target and image corresponds to the distance between the peak of the antenna lobe and the first null. The pattern has converged to its final value by the tenth iteration.

Figure 4 corresponds to a half-beamwidth separation between the target and image. An improvement in image discrimination can be seen on each iteration until the final value is reached. A close examination of the plots reveals that little main-lobe distortion occurs; however, the primary effect is a shifting of the main-lobe axis. The final alignment of the radiation pattern is such that the target is strongly favored while at the same time the image is illuminated minimally.

For the low-angle-tracking problem, a more realistic ratio of target strength to image strength is 1 to 0.9. This case is plotted in Fig. 5 for a half-beamwidth separation between target and image. Convergence of the pattern is considerably slower than in Figs. 3 and 4 where the relative strengths are 1 to 0.5. By iteration 30 the discrimination against the

*For an S-band (λ = 0.33 ft) radar and a 6.6 ft aperture, this corresponds to a range of 22 naut. mi.

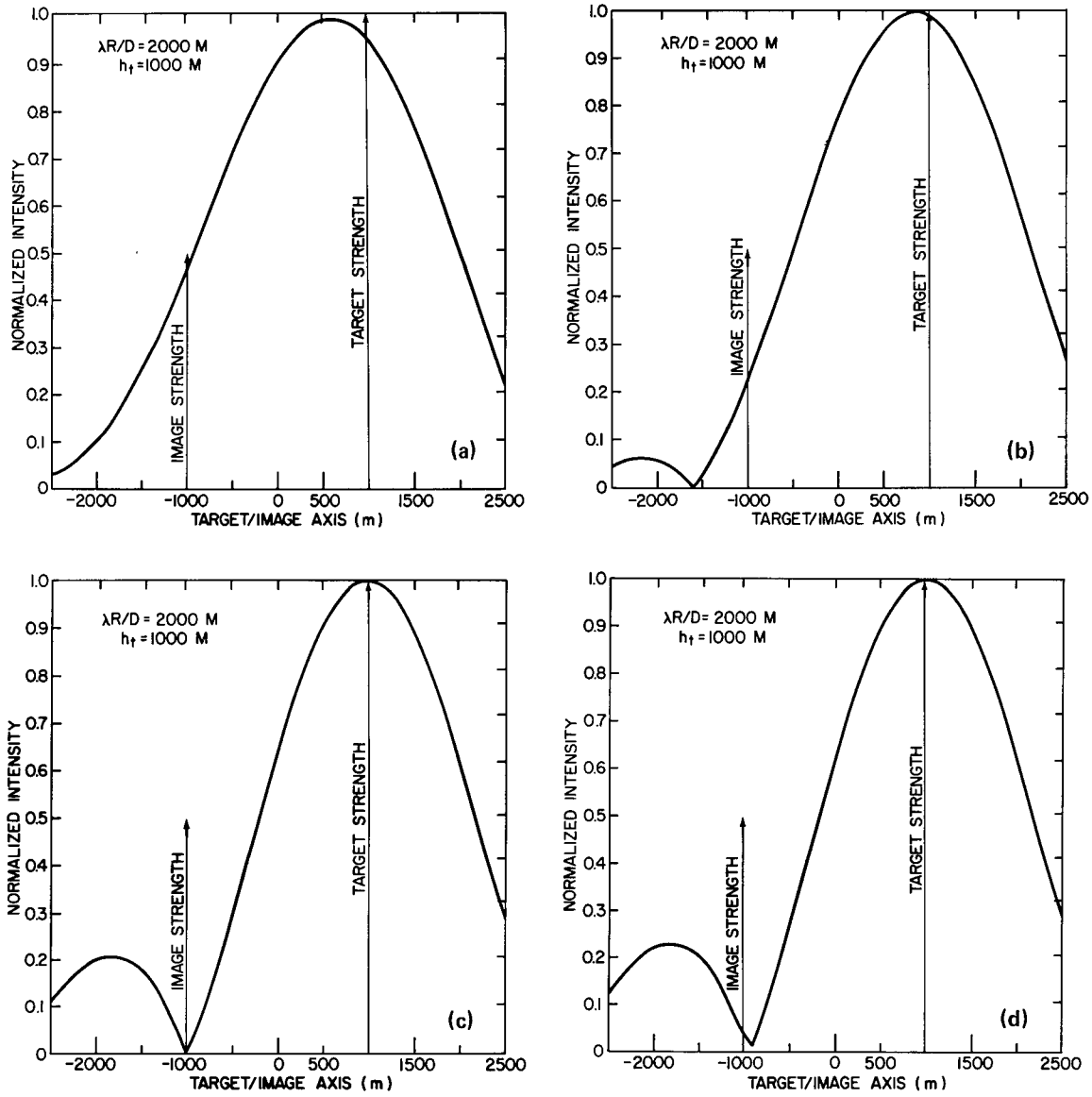

Fig. 3 — Pattern of a self-focusing antenna when the target/image spacing is one beamwidth. (a) One iteration, (b) Two iterations, (c) Five iterations, (d) Ten iterations.

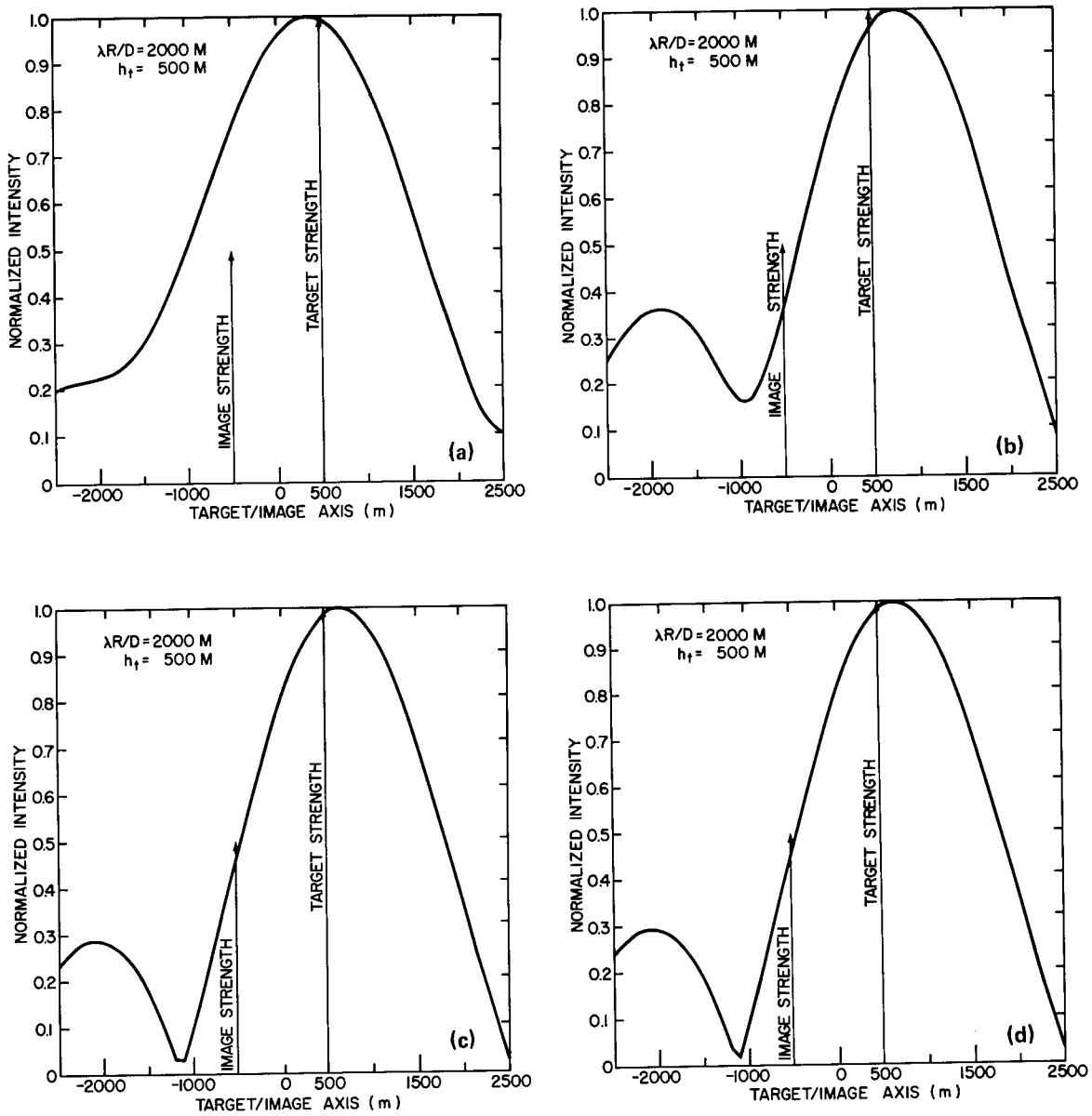

Fig. 4 — Pattern of a self-focusing antenna when the target/image spacing is half beamwidth. (a) One iteration, (b) Two iterations, (c) Five iterations, (d) Ten iterations.

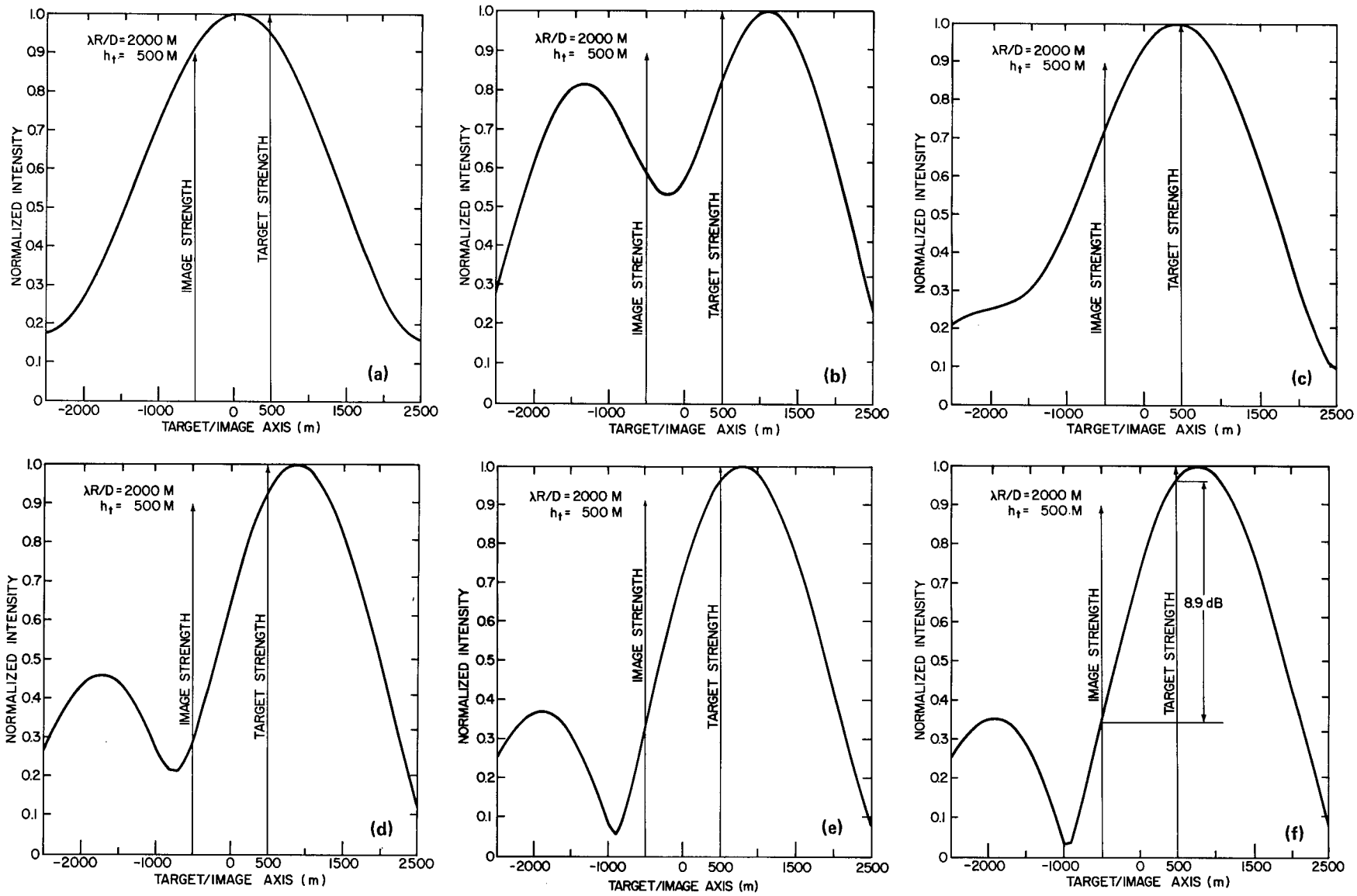

Fig. 5 — Pattern of a self-focusing antenna when the target/image spacing is half beamwidth and the relative image strength is 0.9. (a) One iteration, (b) Two iterations, (c) Five iterations, (d) Ten iterations, (e) Twenty iterations, (f) Thirty iterations.

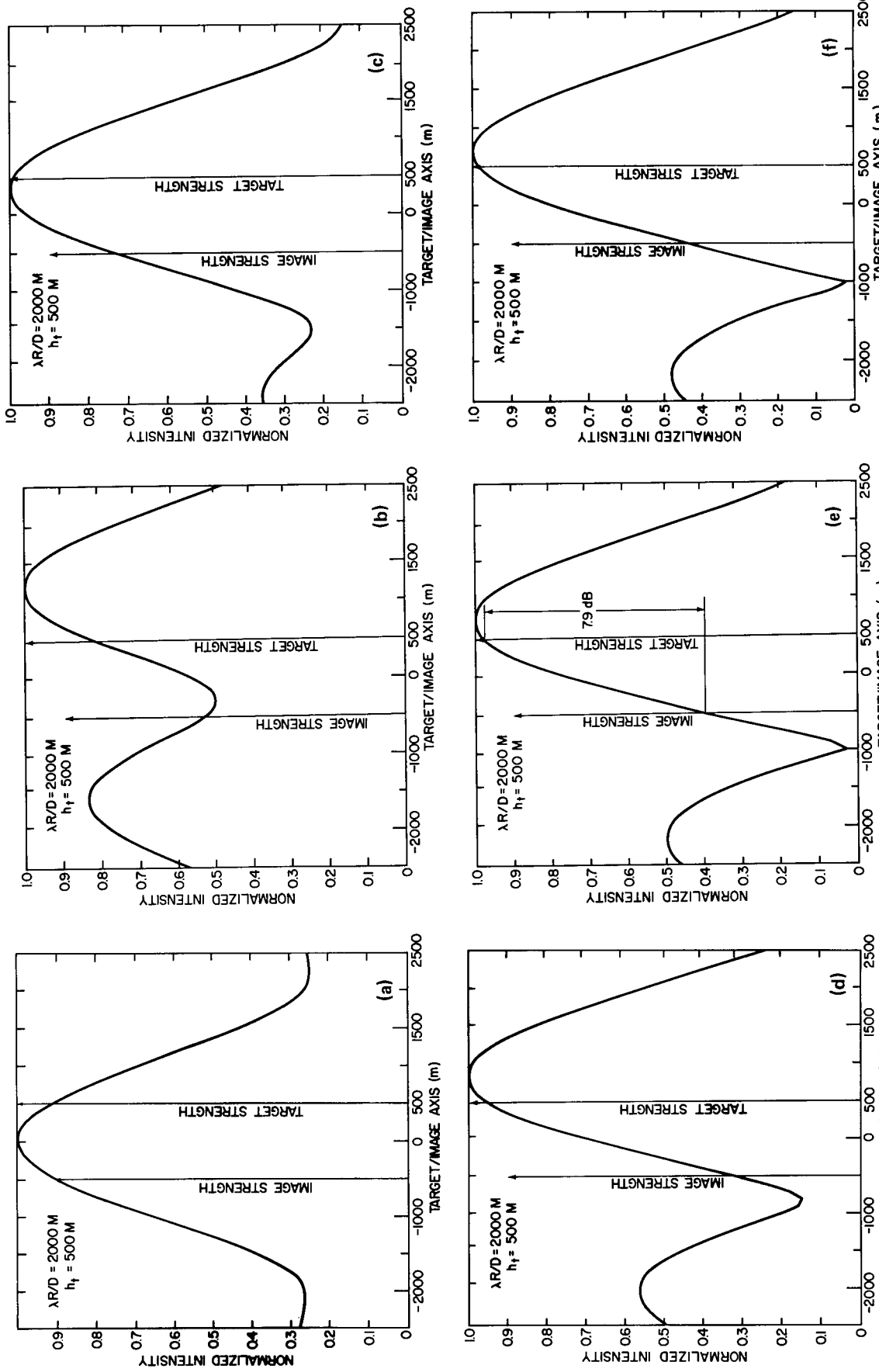

Fig. 6 — Pattern for self-focusing applied to two subapertures. The target/image spacing is half-beamwidth and the relative image strength is 0.9. (a) One iteration, (b) Two iterations, (c) Five iterations, (d) Ten iterations, (e) Twenty iterations, (f) Twenty-nine iterations.

image is 8.9 dB. Although not shown in the figure, after iteration 29 the discrimination was 8.4 dB, and the effect is somewhat oscillatory. The final value would be about 8.7 dB. It is interesting that this is somewhat better than the final value in Fig. 4d, which was 6.75 dB.

Finally, in Fig. 6 the results obtained for the two subapertures are shown. The results in Fig. 6 are extremely encouraging in that the final value of discrimination is about 7.5 dB or only about 1.25 dB worse than the results for the full-aperture case of Fig. 5. Convergence is slow in Fig. 6, but it does not appear to be any slower than in Fig. 5. There is some cause for concern in Figs. 5 and 6 in that a high side lobe appears below the image in both cases. The effect of this side lobe is to increase the sea-clutter level. It is possible that this clutter may correspond to a range cell outside the cell of interest, in which case the effect may be negligible. On the other hand, the effect of the clutter on the focused pattern itself is unknown.

CONCLUSIONS

It has been demonstrated that a self-focusing antenna can discriminate against the weaker of two targets even when the target spacing is such that both targets are well within the beamwidth of the antenna. Furthermore, the results obtained indicate that it may be possible to achieve good image discrimination in low-angle tracking using two subapertures rather than phasing the individual elements of an array.

The results of this brief study are not sufficient to conclude that a self-focusing antenna would be useful for low-angle tracking. This writer feels that two additional questions must be considered before even the most tentative conclusion can be drawn. First, the effect of target motion needs to be considered. This can be investigated by a rather straightforward modification to the existing computer program.

The more critical question regards the actual tracking error. To investigate this question, a suitable tracking algorithm must be developed and analyzed. At this point it is not perfectly clear how to use the self-focusing technique most effectively. However, an approach which appears promising is to use self-focusing in conjunction with monopulse: the target would be illuminated by the self-focusing antenna, and tracking could be accomplished by a separate monopulse system operating in a receive-only mode.

ACKNOWLEDGMENT

This study owes its existence to Dr. M. I. Skolnik. The idea of using self-focusing for low-angle tracking is his, and I am grateful for having had the opportunity to work on it.

My deepest appreciation goes to Dr. W. M. Waters. During the brief period of this study, I spent several hours in discussion with him. His explanations and interest were indispensable. It was in fact his computer program which I used with minor modifications, and the mathematical development presented here is from his work, Ref. 5.

REFERENCES

1. J.H. Dunn and D.D. Howard, "Target Noise," in *Radar Handbook*, M. I. Skolnik, Ed., McGraw-Hill, New York, 1970.

2. D.D. Howard, J.T. Nessmith, and S.M. Sherman, "Monopulse Tracking Errors Due to Multipath: Causes and Remedies," *IEEE EASCON '71 RECORD*, Institute of Electrical and Electronic Engineers, New York, 1971, p. 175.

3. M.I. Skolnik and D.D. King, "Self-Phasing Array Antennas," IEEE Trans. Ant. and Prop. **AP—12**, No. 2, 142 (1964).

4. B.A. Sichelstiel, W.M. Waters, and T.A. Wild, "Self-Focusing Array Research Model," IEEE Trans. Ant. and Prop. **AP—12**, No. 2, 150 (1964).

5. W.M. Waters, "Adaptive Radar Beacon Forming," IEEE Trans. Aero. and Elec. Sys. **AES—6**, No. 4, 503 (1970).

Appendix

COMPUTER SIMULATION PROGRAM FOR THE SELF—FOCUSING PROBLEM

```
      PROGRAM C
      COMPLEX         CI(60),CA(60),A(60),AO,GAMMA,DUM,Z(60,60),FAC(5,5)
     1,AUX(60,60),RHO(60),BUM
      DIMENSION X(60),U(60),COSPHI(60,60),SINPHI(60,60),ANORM(60),
     1AMAG(60),NPLOT(20),PLTARRAY(254)
      CALL PLOTS(PLTARRAY,254,1)
      READ 2,XMIN,XMAX,DELX
    2 FORMAT(6F10.2)
      READ 2,UMIN,UMAX,DELU
      READ 3,R,NMAX,WLAM
    3 FORMAT(F10.2,I5,F10.2)
      READ 4,ICASE,NP,(NPLOT(I),I=1,NP)
    4 FORMAT(10(I5))

      ICASE=CAWE NO.,NP=NO. OF PLOTS,NPLOT=ITERATON FOR PLOTS,NMAX=NO OF IT.

      PI=3.14159265
      AO=(1.,0.)
      GAMMA=(1.,0.)

      COMPUTE X-ARRAY

      PRINT 5,XMIN,XMAX,DELX
    5 FORMAT(1H1,15X,*XMIN=*,F10.2,15X,*XMAX=*,F10.2,15X,*DELX=*,F10.2)
      PRINT 6,UMIN,UMAX,DELU
    6 FORMAT(//15X,*UMIN=*,F10.2,15X,*UMAX=*,F10.2,15X,*DELU=*,F10.2)
      XLOD=WLAM/(XMAX-XMIN)
      ELANG=UMAX/R
      XLUM=XLOD*R
      PRINT 7,R,NMAX,WLAM
    7 FORMAT(//15X,*RANGE=*,F10.2,*METERS      NMAX=*,I3,5X,*LAMBDA=*,
     1F6.2,*CM*)
      PRINT 8,XLOD,ELANG,XLUM
    8 FORMAT(//10X,*LOD=*,E10.3,5X,*EL ANGLE=*,E10.3,5X,*LR/D=*,E10.3)
      I=1
      X(I)=XMIN
   10 I=I+1
      X(I)=X(I-1)+DELX
      IF(X(I)-XMAX)10,11,11
   11 IMAX=I

      COMPUTE U-ARRAY$JMAX

      NTARG=0
      J=1
      U(J)=UMIN
      RHO(J)=(0.,0.)
   12 J=J+1
      U(J)=U(J-1)+DELU
      IF(U(J).EQ.-500.)14,153
  153 IF(U(J).EQ.500.)15,60
   15 RHO(J)=(1.,0.)
      JTARG=J
      GO TO 16
   14 RHO(J)=(.9,0.)
      JIMAG=J
   16 NTARG=NTARG+1
      GO TO 17
   60 RHO(J)=(0.,0.)
```

```
17 IF(U(J)-UMAX)12,18,18
18 JMAX=J

  COMPUTE SIN$COS OF PHI

   JHALF=JMAX/2
   DO 19 I=1,IMAX
   DO 19 J=1,JMAX
   PHI=P1*2./WLAM*SQRT(R**2+(X(I)-U(J))**2)
   IF(J.LT.JHALF)PHI=PHI+P1
   COSPHI(I,J)=COS(PHI)
19 SINPHI(I,J)=SIN(PHI)

    COMPUTE COMP ES VALUES OF GAMMA

   DO 20 I=1,IMAX
   DO 20 J=1,JMAX
   DUM=CMPLX(COSPHI(I,J),SINPHI(I,J))
20 Z(I,J)=GAMMA*DUM

    CLEAR AN(U) ARRAY ONCE ONLY FOR ALL ITERATIONS

   DO 21 J=1,JMAX
21 A(J)=(0.,0.)

   CLEAR IN(U) ARRAY (TARGET REFLECTION) AND RECEPTION ARRAYS FOR EACH
  ITERATION

   DO 22 J=1,JMAX
22 CI(J)=(0.,0.)
   DO 23 I=1,IMAX
23 CA(I)=(0.,0.)

   COMPUTE FIRST ITERATION OF AN(U),IN(U)$AN(X)

   IHALF=IMAX/2
   N=1
   DO 24 J=1,JMAX
24 CI(J)=RHO(J)*AO
   DO 25 I=1,IMAX
   DO 25 J=1,JMAX
25 CA(I)=CA(I)+CI(J)*Z(I,J)
  EQ 1 IN WATERS'1Z
   BUM=(0.,0.)
   DUM=(0.,0.)
   DO 128 I=1,IHALF
128 DUM=DUM+CA(I)
   ME=IHALF+1
   DO 129 I=ME,IMAX
129 BUM=BUM+CA(I)
   BUM=CONJG(BUM)/(IMAX-IHALF)
   DUM=CONJG(DUM)/IHALF
   DO 130 I=1,IHALF
130 CA(I)=DUM
   DO 131 I=ME,IMAX
131 CA(I)=BUM
   DO 26 J=1,JMAX
   DO 26 I=1,IMAX
26 A(J)=A(J)+CA(I)*Z(I,J)
```

```
      GO TO 32
       CLEAR IN(U)$AN(X) ARRAYS $ ITERATE
   37 DO 27 J=1,JMAX
   27 CI(J)=(0.,0.)
      DO 28 I=1,IMAX
   28 CA(I)=(0.,0.)
      DO 29 J=1,JMAX
   29 CI(J)=RHO(J)*A(J)
      DO 30 I=1,IMAX
      DO 30 J=1,JMAX
   30 CA(I)=CA(I)+CI(J)*Z(I,J)
      BUM=(0.,0.)
      DUM=(0.,0.)
      DO 138 I=1,IHALF
  138 DUM=DUM+CA(I)
      DO 139 I=ME,IMAX
  139 BUM=BUM+CA(I)
      DUM=CONJG(DUM)/IHALF
      BUM=CONJG(BUM)/(IMAX-IHALF)
      DO 140 I=1,IHALF
  140 CA(I)=DUM
      DO 141 I=ME,IMAX
  141 CA(I)=BUM
      DO 40 J=1,JMAX
   40 A(J)=(0.,0.)
      DO 31,J=1,JMAX
      DO 31 I=1,IMAX
   31 A(J)=A(J)+CA(I)*Z(I,J)
   32 PRINT 1003,ICASE,NTARG,N
 1003 FORMAT(14X,*ADAPTIVE ARRAY PHASING PROBLEM*,//,17X,*CASE*,I2,2X,I3
     1,*POINT TARGERTS*,//20X,*ITERATION NUMBER*,I3,//13X,*U(J)*,17X,
     2*NORMALIZED AN(U)*,//)
      AMAX=0.
      DO 33 J=1,JMAX
      AMAG(J)=CABS(A(J))
   33 AMAX=MAX1F(AMAG(J),AMAX)

      NORMALIZE AN(U) $ PRINT OUT U $ AN(U)

      DO 34 J=1,JMAX
      ANORM(J)=AMAG(J)/AMAX
   34 CONTINUE
      DISCRM=20.*ALOG10(ANORM(JTARG)/ANORM(JIMAG))
      PRINT 1005,DISCRM
 1004 FORMAT(11X,F8.2,10X,E20.8)
 1005 FORMAT(5X,*IMAGE DISCRIMINATION=*,F6.2,*DB*)
      DO 50 I=1,NP
      IF(N.EQ.NPLOT(I))51,50
   51 CALL GRAPHPLT(ANORM,PLTARRAY,JMAX)
   50 CONTINUE
      IF(N-NMAX)35,36,36
   35 N=N+1
      GO TO 37
   36 CONTINUE
      CALL STOPPLOT
      END
```

```
      SUBROUTINE GRAPHPLT(ANORM,PLTARRAY,JMAX)
      DIMENSION ANORM(1),PLTARRAY(254)
      X=0.
      Y=0.
      IP=-3
      CALL PLOT(X,Y,IP)
      IP=2
      DO 100 I=1,10
      X=X+1.
      CALL PLOT(X,Y,IP)
      Y=.1
      CALL PLOT(X,Y,IP)
      Y=0.
      CALL PLOT(X,Y,IP)
  100 CONTINUE
      IP=3
      X=0.
      Y=0.
      CALL PLOT(X,Y,IP)
      DO 200 I=1,10
      IP=2
      Y=Y+1.
      CALL PLOT(X,Y,IP)
      X=.1
      CALL PLOT(X,Y,IP)
      X=0.
      CALL PLOT(X,Y,IP)
  200 CONTINUE
      CALL PLOT(4.,0.,3)
      CALL PLOT(4.,9.,2)
      CALL PLOT(4.,0.,2)
      CALL PLOT(6.,0.,3)
      CALL PLOT(6.,10.,2)
      CALL PLOT(6.,0.,2)
      X=0.
      IP=3
      Y=0.
      CALL PLOT(X,Y,IP)
      DO 300 J=1,JMAX
      IP=2
      X=.2*(J-1)
      Y=10.*ANORM(J)
      CALL PLOT(X,Y,IP)
  300 CONTINUE
      CALL PLOTS(0,0)
      CALL PLOTS(0,0)
      RETURN
      END
```

Security Classification

DOCUMENT CONTROL DATA - R & D

(Security classification of title, body of abstract and indexing annotation must be entered when the overall report is classified)

1. ORIGINATING ACTIVITY (Corporate author)	2a. REPORT SECURITY CLASSIFICATION
Naval Research Laboratory Washington, D. C. 20375	Unclassified
	2b. GROUP

3. REPORT TITLE

USE OF A SELF–FOCUSING ANTENNA FOR LOW–ANGLE TRACKING

4. DESCRIPTIVE NOTES (Type of report and inclusive dates)

A final report on one phase of a continuing problem.

5. AUTHOR(S) (First name, middle initial, last name)

James H. Hughen

6. REPORT DATE	7a. TOTAL NO. OF PAGES	7b. NO. OF REFS
June 28, 1973	18	5

8a. CONTRACT OR GRANT NO.	9a. ORIGINATOR'S REPORT NUMBER(S)
NRL Problem R02-59	
b. PROJECT NO.	NRL Report 7579
RF-12-151-402-4015	
c.	9b. OTHER REPORT NO(S) (Any other numbers that may be assigned this report)
d.	

10. DISTRIBUTION STATEMENT

Approved for public release; distribution unlimited.

11. SUPPLEMENTARY NOTES	12. SPONSORING MILITARY ACTIVITY
	Department of the Navy Office of Naval Research Arlington, Va. 22217

13. ABSTRACT

The response of a self-focusing antenna to two closely spaced point targets is investigated. The geometry simulated corresponds to the radar tracking of a low-flying target over a reflective surface. In one case the antenna consists of a vertical linear array of elements. When the conjugates of the incident signals are retransmitted at each element, after several iterations the antenna radiation pattern introduces significant discrimination against the weaker of the two unresolvable point targets. In the other case the same aperture is divided into two equal subapertures, and conjugate reflections are applied to the two subapertures rather than to each element. It is found that very nearly the same weak-target discrimination results. The implications of these results with regard to low-angle tracking are discussed.

DD FORM 1 NOV 65 1473 (PAGE 1)

S/N 0101-807-6801

Security Classification

14. KEY WORDS	LINK A		LINK B		LINK C	
	ROLE	WT	ROLE	WT	ROLE	WT
Self-focusing antenna Low-angle tracking Angular resolution						